PHASER – A Phase-Shifting Antenna for Low-Power Directional Communication

Leo Selavo
Institute of Electronics and Computer Science, Latvia

Dhruv Vyas, Moosa Yahyazadeh, Octav Chipara
University of Iowa, USA

***Abstract*—This paper describes the design and empirical evaluation of PHASER — a mote prototype for low-power directional communication in wireless sensor networks. PHASER has a modular design that includes three components: a low-power radio, an RF signal processing chip, and two off-the-shelf antennas. Directional communication is achieved by splitting the output signal from the low-power radio chip and controlling programmatically the phase of each signal as it transmitted to each antenna. The net effect of controlling the phase of the signals is that they generate patterns of constructive and destructive interference as signals propagate. PHASER is well-suited for wireless sensor networks as it does not require heavyweight signal processing techniques and consumes minimal additional energy.**

We have extensively evaluated the performance of five PHASER prototypes. Empirical results clearly demonstrate that changing the phase configuration of PHASER can generate diverse anisotropic radiation patterns. The diverse radiation patterns may be used to increase the signal strength at an intended receiver. Our data indicates that the signal strength of a link can be increased by at least 13 dBm. We also show it is possible to take advantage of the anisotropy of the radiation patterns to facilitate spatial reuse. More importantly, we show that the quality of the links from the same PHASER mote has a common pattern that can be predicted using a simple model. Our evaluation shows that model introduces an median absolute error of about 2 dBm. The model may be used for realistic simulations or integrated into protocol stacks to identify the phase configurations that improve link quality or spatial reuse.

I. Introduction

The wireless sensor network (WSN) community has extensively studied low-power communication when nodes are equipped with omnidirectional antennas. However, in contrast to omnidirectional antennas, smart directional antennas can be controlled by software to transmit signals in a preferential direction to create multiple radiation patterns. The diversity of radiation patterns can be exploited to selectively increase (or decrease) the signal at a receiver and improve spatial reuse. This basic capability can be a foundation for building the next generation of low-power wireless stacks that can extend the reach of low-power wireless communication by improving throughput, energy-efficiency, reliability, and security.

The design of directional antennas for WSNs faces three challenges that are poorly addressed by existing antenna designs. First, WSN nodes typically trade-off computation and memory resources in favor of energy efficient micro-controllers. Accordingly, a directional antenna solution must employ lightweight signal processing techniques to keep energy consumption to a minimum. Additionally, directional communication must introduce a minimal processing overhead given the paucity of computational resources. Second, WSN nodes tend to be small and, as a result, their antennas must also be small. Bulky antenna designs would significantly limit the extent to which they may be deployed. Finally, directional antennas must be simple to manufacture. Ideally, a directional antenna design should use off-the-shelf components that may be put together with minimal effort.

The performance of Wi-Fi networks can be significantly improved using directional communication techniques such as MIMO. Unfortunately, Wi-Fi networks are less energy efficient than 802.15.4 radios at low data rates. Incorporating MIMO techniques that require heavy signal processing of multiple radio signals would only reduce its efficiency in this operating regime. A number of alternatives that are better suited for WSN applications have been proposed (see Section IV for details). A common approach to achieving directional communication are electronically switched parasitic element antennas. This type of antennas has a central active element that is surrounded by parasitic elements. A software driver controls the directionality of the radiated pattern by either grounding or isolating the parasitic elements and thus reflecting or directing the RF signal. This design was implemented by the SPIDA antenna whose link properties have been studied in [1]. A limitation of SPIDA is that its performance is significantly affected by the antenna geometry.

This paper aims to improve the directional communication for low powered distributed systems and makes the following contributions: (1) We describe PHASER — a prototype for low-power directional communication that is easy to build and has low power consumption. (2) We extensively evaluate PHASER by measuring and characterizing the diversity and extent of radiation patterns using two new metrics: directional benefit and spatial reuse index. (3) We propose a computationally efficient and accurate model for predicting the quality of links of a PHASER mote at different receivers.

PHASER's design is modular and has three components: a low-power radio chip, an RF signal splitter and phase shifter chips, and off-the-shelf antennas. Directional communication is achieved by splitting the output signal from

the low-power radio chip. A hardware chip is used to control the phase of the signals transmitted to the two antennas. A software driver is used to programmatically control the phase of the signals. The net effect is that the signals generate patterns of constructive and destructive interference as signals propagate. If the resulting antenna patterns are diverse, then this can provide an approach to improving wireless communication performance. In contrast to SPIDA, our design is simpler as it uses off-the-shelf components and does not require complex manufacturing. It is our hope that by creating a simpler and open-source design, we will catalyze research on directional communication in WSNs.

The properties of the PHASER motes were measured outdoors and indoors using testbed composed of 16 TelosB motes. The results of the empirical study show that by changing the phase configuration, PHASER can create significantly different radiation patterns both indoors and outdoors. We introduce two metrics – directional benefit and spatial reuse index – to quantify the benefit of having multiple radiation patterns compared to a single one (as it is the case with omnidirectional antennas). The directional benefit capture PHASER's ability to improve the link quality to a receiver at a given orientation. Our analysis shows that the quality of a link can be improved by at least 13 dBm. The spatial reuse index is defined as the fraction of orientations of the transmitter for which spatial reuse is possible. Considering two receivers, R and P, we say that it is possible to transmit concurrently to R and P if the difference in the signal strength at R and P exceeds a reuse threshold. Our analysis indicates that when the threshold is set to 6 dBm, the spatial reuse index is in the range 40% – 80%. The spatial reuse index decreases linearly with the increase in the reuse threshold. This suggests that PHASER is effective in creating spatial reuse opportunities.

The last part of the empirical study focuses on exploring the link quality properties. We observe that changing the phase configuration can effectively control the quality of the link as measured by receive signal indicator, link quality indicator, and packet reception rate. We defined the phase matrix to be a matrix whose rows and columns indicate the phases with which signals are transmitted and the entries indicate the RSSI for a specific antenna configuration. We show that if we use the phase matrix of a node as a template, we can reconstruct the phase matrices of any other node applying a simple transformation: (1) shifting the phases to account for shifts in the phase matrix and (2) scaling the obtained matrix to account for differences in RSSI caused by the nodes having different distances to the receiver. The median accuracy error varies between nodes but is at most 2 dBm. This model can be effectively exploited to find the appropriate phase patterns to both improve link quality and identify spatial reuse opportunities. Estimating the phase shifts and scaling parameters is sufficient to characterize the observed RSSI at all nodes in line-of-sight conditions.

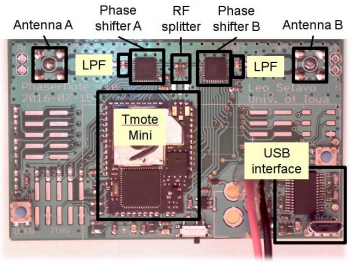

Figure 1: PHASER board and block diagram. The board has Tmote-mini with a MSP430 MCU and CC2420 radio, RF splitter, phase shifter, low pass filter, and antenna connectors.

II. PHASER Hardware Prototype

The PHASER module has been designed around Tmote Mini module that includes a TI MSP430 microcontroller and a CC2420 RF transceiver chip with a pin for external antenna connection (see Figure 1). The pin is connected to a power splitter that divides the RF signal in two. Each of the split signals is fed into a digitally controllable RF phase-shifter chip PE44820. Each of the two chips is controlled by digital signals from the Tmote Mini allowing to shift the phase in 1.4-degree increments, a total of 256 configurations for each antenna [2]. According to the datasheet, phases may be controlled within ± 3 degrees and the settling time is 365ns within 2 degrees of final value. Finally, a low-pass filter with a cut-off frequency of 2.4GHz is applied to the RF signal before it is being fed into two monopole antennas that are $\lambda/2$ apart. The antennas are mounted on a round ground plane that is extended with a ground skirt.

The design is economical with respect to the energy consumption. Changing the phase configuration is no more than changing the logical value on 9 pins for each of the two phase-shifter chips. The two phase-shifters add a total of 0.4mA to the typical Tmote Mini current consumption of 22mA with the radio transceiver active. There is no additional signal processing requiring more energy, other than what the communication protocol determines by changing the configurations and the transmission power.

III. Empirical Study

The focus of the empirical study is to demonstrate that phase-shifting antennas are an effective approach to supporttng directional communication in WSNs. We will evaluate PHASER's ability to (1) transform low-quality links into high-quality links and (2) enable spatial reuse by changing antenna configurations. To this end, we have carried out an extensive study using five PHASER motes and a testbed consisting of 16 TelosB motes. Specifically, the empirical study will focus on the following questions: (1) What is the impact of changing PHASER configuration on directional communication? (2) What is the impact of using different off-the-shelf antennas on PHASER's performance? (3) How

can we identify a PHASER configuration that maximizes link quality of spatial reuse?

Answering these questions will provide a sound basis for understanding the challenges and opportunities of using phase-shifting antennas for supporting directional communication in WNSs. The results complement prior work on supporting directional communication in WSNs using electronically switched antennas. A unique challenge to using a phase-shifting antenna is the high number of potential configurations; PHASER has a total of 65,536 configurations compared to only 64 in the case of SPIDA. Our analysis aims to both analyze the impact of changing the configuration as well as provide insights on how appropriate configurations can be identified to maximize the benefits of directional communication.

A. Methodology

We have evaluated the performance of PHASER using two type of experiments: radiation pattern measurements and link quality measurements. Experiments were conducted either outdoors on an empty rugby field or indoors in a 5m $\times$ 7m room. In order to perform the indoor experiments, we have constructed a sixteen mote testbed. The motes are installed on a wooden frame that is elevated at 2.5m off the floor. TelosB motes are equipped with a TI MSP430 micro controller and CC2420 RF transceiver. The PHASER mote is placed is elevated on a tripod slightly below the level of the TelosB motes. There are minimal line-of-sight obstacles between the PHASER and the TelosB motes. Signal propagation is subject to multi-path effects and potential interference caused by other running equipment such as computers and lighting.

In order to measure the radiation patterns, we have constructed a digitally controllable turntable. The turntable responds to commands over a wireless link that directs a stepper-motor to turn the table to a specified angle. The turntable may be controlled in increments of 1.8 (there are 200 positions for a full circle). The mote under study is placed on top of the turntable. The motor is powered down during experiments to eliminate a source of potential interference. In order to evaluate the transmission radiation pattern, the PHASER mote transmits sequences of 100 packets for a turntable angle and antenna configuration. An antenna configuration includes the phases of the signals transmitted to the two antennas of the PHASER mote. All the considered antenna configurations are evaluated prior to changing the angle of the transmitter. The sixteen TeslosB motes are used to record the receiver signal strength indicator (RSSI) and link quality indictor (LQI) of each received packet. All the radiation pattern experiments are carried out on channel 26 that does not overlap with the existing Wi-Fi and packets are transmitted at -15 dBm.

We constructed six PHASER prototypes one of which we have identified to be faulty. We will refer to each of the prototypes using letters `A` through `F`. We have tested PHASER in combination with whip antennas (108mm, 2 dBi). We control one or both of the phases of signals sent to the antennas of PHASER. Therefore, a configuration $c = (\phi_A, \phi_B)$ controls the phases of the signals transmitted to antennas A and B of PHASER. An 8-bit number is used to represent the phase shift of a signal. Each antenna has a phase shift configuration option with 256 possible shift values distanced at 1.4 degrees each. Since we have 2 antennas with a phase shifter for each, the total number of configurations is 65536.

B. Metrics

The degree to which PHASER can support directional communication is measured according to two metrics: directional benefit and spatial reuse index. The directional benefit assesses the degree to which PHASER can transform a low-quality link into a high-quality link by changing the phase configuration. Accordingly, consider measuring the quality of a link established between PHASER and a receiver, when the PHASER mote is oriented at γ degrees on the turntable. The directional benefit is defined as:

$$B(\gamma) = \max_{c \in \mathcal{C}} RSSI(c, \gamma) - \min_{c \in \mathcal{C}} RSSI(c, \gamma) \qquad (1)$$

where $RSSI$ is the received signal strength of the receiver measured in decibels and $\mathcal{C}$ is the set of antenna configurations. The benefit of using a directional antenna for a given orientation of the receiver can be improved by B dBm over the worst-case RSSI. The mean directional benefit is computed as the average benefit over orientations $\gamma \in \Gamma$, where Γ is the set of the possible orientation of PHASER on the turntable.

$$\bar{B} = \sum_{\gamma \in \Gamma} B(\gamma)/|\Gamma| \qquad (2)$$

The spatial reuse index is designed to capture PHASER's ability to create spatial reuse opportunities. To this end, let us consider the case when PHASER uses a configuration $c = (\phi_A, \phi_B)$ to transmit packets to a target receiver R oriented at γ_R degrees. We say that another receiver P oriented at γ_P degrees may be reused when the difference in the signal strengths at the two receivers exceeds a reuse threshold value T i.e., $RSSI(c, \gamma_R) - RSSI(c, \gamma_P) \geq T$. Formally, we defined the indicator $I(\gamma_R, \gamma_P, T)$ to capture the orientations for which spatial reuse is possible given a threshold T.

$$I(\gamma_R, \gamma_P, T) = \begin{cases} 1 & \exists c \in \mathcal{C} \text{ s.t.} \\ & \quad RSSI(c, \gamma_R) - RSSI(c, \gamma_P) \geq T \\ 0 & \text{otherwise} \end{cases}$$

The spatial reuse index (SRI) for a given threshold T is computed by considering all possible locations of R and P around the circle:

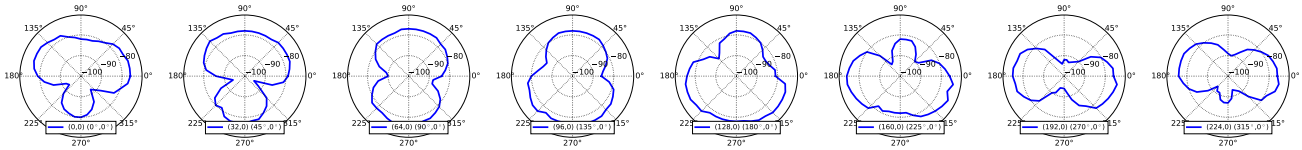

Figure 2: Outdoor radiation patterns when the phase of antenna B is 0 and the phase of antenna A is varied from 0 to 255.

$$SRI(T) = \frac{|\{(\gamma_R, \gamma_P) \in \Gamma \times \Gamma \mid I(\gamma_R, \gamma_P, T) = 1\}|}{|\Gamma|^2} \quad (3)$$

SRI has a value between 0% – 100% indicating the fraction of orientations where reuse is possible. A detailed example of computing the SRI is discussed later in this section.

C. Radiation Pattern Experiments

1) Radiation Patterns: The initial experiment is designed to evaluate the performance of PHASER in an environment with minimal external interference and multi-path effects. The experiment was carried out on a rugby field where the turntable was placed in the middle of the field. The PHASER was powered using an external battery for the duration of the experiment. The configuration of PHASER was varied by holding the phase for antenna B constant and varying the phase of antenna A from 0 to 255 in increments of 32.

The radiation patterns observed during the experiment are shown in Figure 2. The figure clearly shows that changing the phase configuration has a significant impact on the observed radiation patterns. Most of the radiation patterns tend to be anisotropic displaying preferential propagation in a given direction. For example, when the PHASER is configured to $(192, 0)$ the radiation pattern resembles of horizontal "figure 8". The main lobes of the antenna are pointed towards $0°$ and $180°$. Conversely, the "nulls" of the antenna point are at $90°$ and $270°$, respectively.

The change of the phase configuration has a predictable behavior. When the phase of antenna A, ϕ_A is 0, the main lobe of the antenna is pointed at $90°$. Increasing ϕ_A to 32 and later to 64 results in increasing the size of the lobe pointing towards $270°$ and shrinking of the lobe pointing at $90°$. When $\phi_A = 64$, the radiation pattern looks like a vertical "figure 8". Increasing ϕ_A to 96, 128, and 160 shows a slow transition from having lobes pointing to $90°$ and $270°$ to lobes pointing to $0°$ and $180°$. When ϕ_A is 192, the radiation pattern looks like a horizontal "figure 8".

The above sequence of figures clearly shows we can create different radiation patterns by controlling the phases of the signals. The key is to appropriately select the radio pattern depending on your communication goal. For example, in the case you want to communicate with that has an orientation of $90°$, you may want to use configuration $(64, 0)$. Additionally, this configuration opens opportunities for spatial reuse. For example, other nodes that are located at the "nulls" of the radiation pattern (i.e., $0°$ or $180°$) may be used as other transmissions. Alternatively, if you consider the security concerns due to eavesdropping, a transmission using this pattern would leak the minimal amount of information to the same positions.

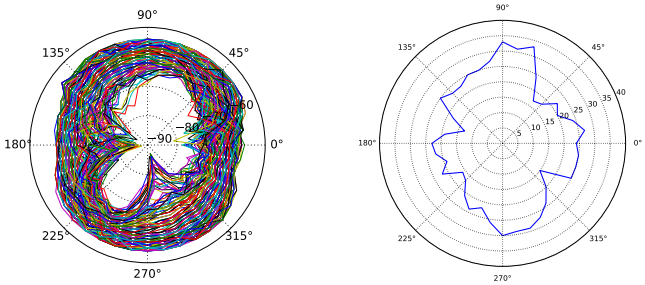

(a) Radiation patterns (b) Directional benefit

Figure 3: Patterns and directional benefit for node 1.

Results 1: A fixed configuration creates a radiation pattern that is anisotropic. Changing the phase configuration creates diverse radiation patterns.

2) Directional Benefit: Next, we evaluate the directional benefit provided by PHASER. In this set of experiments, the configuration of PHASER is changed by varying the phases ϕ_A and ϕ_B in range 0 – 255 in increments of 32. Figure 3a plots the radiation patterns for mote `A` as measured by a node 1. The node's directional benefit is computed using equation 1 and plotted in Figure 3b. Essentially, the directional benefit is the difference between the outer hull (i.e., maximum RSS across all configuration) and the inner hull (i.e., minimum RSS across all configuration) of Figure 3a.

The directional benefit of node 1 varies between 13 – 32 dBm depending on the orientation of the PHASER mote. Therefore, a minimum increase of 13 dBm can be observed over the worst-case for any orientation of the transmitter. On average, the directional benefit is 24 dBm, which is an

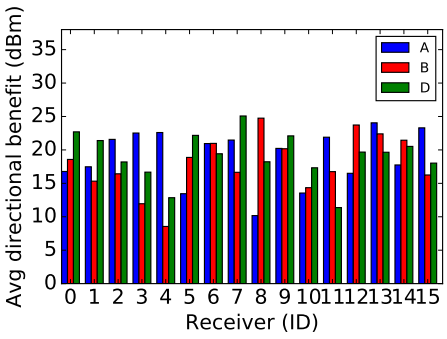

Figure 4: Directional benefit per node

increase in the receive signal strength of over two orders of magnitude. These statistics clearly show the benefit of using directional antennas. In the case of a static antenna, a receiver would have a single anisotropic radiation pattern that could lead to some nodes having low link quality. In contrast, PHASER can increase the RSS by at least 13 dBm and up to 24 dBm on average. We will show that this predicted benefit is materialized in that PHASER can transform low quality link into a high quality link as discussed in Section III-D. Figure 3b shows that the directional benefit is anisotropic. This indicates that the benefit that may be provided by PHASER depends on the orientation of the PHASER mote.

Figure 4 plots the average directional benefit computed for each node in the testbed when different PHASER prototypes are used. The figure indicates that different nodes in the testbed have different average directional benefits ranging from 10 dBm to 24 dBm. We have also evaluated the directional benefit using different PHASER mote. The figure indicates that the nodes that have the largest directional benefit change depending on the PHASER mote that is used. Given that the devices were assembled by hand and are subject to variations in soldering quality these variations in radiation patterns are expected. In order to evaluate the variability across the different PHASER prototype in more detail, we plot the distribution of average directional benefits using a box plot.

Results 2: The directional benefit depends on the orientation of the PHASER mote, the location of the receiver, and the hardware. While the specific benefit observed by a receiver depends on its location, there is only a small variation in the distribution of directional benefits over the entire testbed.

3) Spatial Reuse: A key benefit of directional antennas is that they may allow a greater degree of spatial reuse than traditional omnidirectional antennas. Figure 5a plots the radiation pattern for the phase configuration that maximizes $RSS(c, \gamma_R) - RSS(c, \gamma_P)$, when the target and reuse nodes are placed at γ_R and γ_P, respectively. In our example, there is a clear dip in RSS when $\gamma_P = 90°$ while there is a high RSS at $\gamma_P = 0°$. This example illustrates how PHASER may take advantage of the anisotropy of radiation patterns to foster spatial reuse. We conjecture that if we were to use antennas that have higher anisotropy, PHASER may achieve higher spatial reuse.

Figure 5b plots $RSS(c, \gamma_R) - RSS(c, \gamma_P)$ when $\gamma_R = 0$ and γ_P is varied in the range $0°$ – $360°$. The figure shows that when $\gamma_P \simeq \gamma_R$, it is impossible to have spatial reuse. This is because when nodes P and R have a similar distance and orientation to the transmitter, it is difficult to find a radiation pattern that can simultaneously increase the signal strength P and decrease it at R. Spatial reuse is also not possible when $\gamma_P \simeq 240°$. This is because of the symmetry of the created radiation patterns.

In order to compare the impact of the location of the receiver on spatial reuse, we computed the spatial reuse index for all the nodes in the testbed for different PHASER combinations. We have used a threshold of 6 dBm as previous studies on interference suggest that 6 dBm are sufficient to take advantage of the capture effect. Figure 6a plots the spatial reuse index of different nodes. We remind the reader that the spatial reuse index has values in the range 0% – 100% indicating the fraction of angles for which we expect that spatial reuse is possible. For mote A, the spatial reuse index varies between 43% – 87% covering a large fraction of possible directions. Figure 6b plots the impact of increasing the signal threshold from 4 dBm to 26 dBm. As expected, as we increase the threshold, a smaller fraction of angles allow for spatial reuse. The spatial reuse index decreases linearly as the signal threshold is increased. This behavior is consistent across all the nodes in the testbed. These results indicate that PHASER can create significant opportunities for spatial reuse.

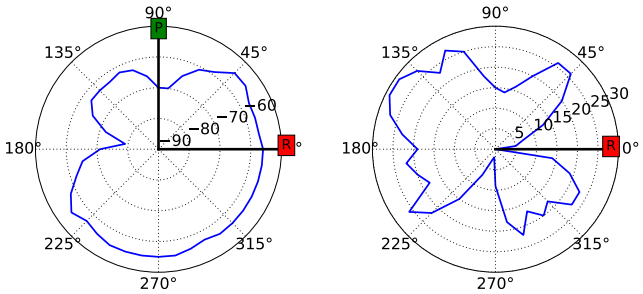

(a) Radiation pattern resulting in the highest SRI when receivers R and R are located at $\gamma_R = 0°$ and $\gamma_P = 90°$.

(b) SRI when the receiver R is at $\gamma_R = 0°$ and the receiver P is at $\gamma_P \in [0°, 360°]$

Figure 5: Spatial reuse index

Results 3: The spatial reuse opportunities depend on the orientation of the PHASER mote and location of receiver. The spatial reuse opportunities decrease linearly with the increase of the spatial reuse threshold.

D. Link Quality Measurements

1) Link Quality: In this section, we turn our attention to analyzing the properties of the links established between the PHASER motes and the nodes comprising the testbed. Our analysis has two goals: (1) demonstrate that varying phase configurations can significantly impact the quality of links and (2) construct a predictive model that characterizes the relationship between the considered links.

Figure 7 characterizes the quality of the link established between PHASER A and node 0. The subfigures plot the PRR, RSSI, and LQI for different phase configurations. The phase configuration is changed by varying the phase of each antenna in the range 0 – 255 in increments of 64. The figure clearly indicates that the quality of the links can be significantly changed by changing the configuration. For example, the PRR can be changed from 0.5% to 99%.

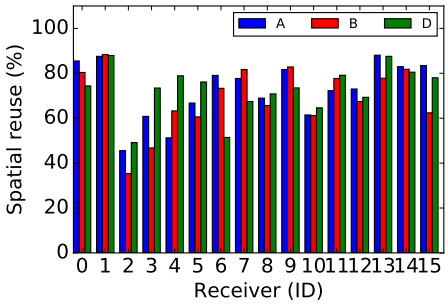

(a) Spatial reuse index measured per node

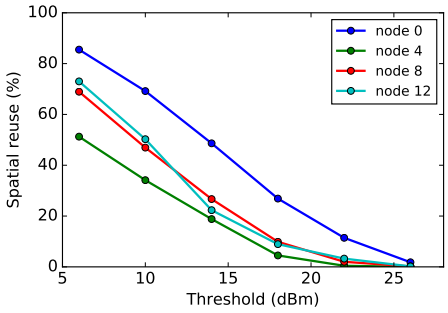

(b) Spatial reuse index of mote A for nodes 0, 4, 8, and 12

Figure 6: Spatial reuse index varies with receiver location and decreases linearly with the signal threshold

Similarly, the RSSI varies in the range -83 dBm to -92 dBm while LQI in the range 75 to 105.

Figure 8 shows the RSSI and PRR of links from PHASER A to the nodes in the testbed. The link statistics of a node are computed by first considering the RSSI and PRR for each phase configuration. The plotted values indicate the minimum, average, and maximum of these average values. The results indicate that changes in the phase configuration can change the average RSSI by 6 – 19 dBm (average 11 dBm). This shows that can PHASER can effectively the RSSI at a receiver within a wide range. However, as shown in Figure 8b the variability in PRR is smaller with a subset of links having high PRR irrespective of phase configuration. The reason for this is that in order to observe packet losses, the PRR of a link must be reduced below a threshold value. In some cases, this is not possible due to the proximity of the receiver to the PHASER mote. This highlights that in dense deployments phase changes must be combined with power control to increase spatial reuse.

Results 4: Phase changes can change the receive signal strength between 6 – 19 dBm. However, the phase change may need to be combined with power control in order to maximize spatial reuse opportunities.

2) A Model for Phase-Shifting Antennas: A key challenge to using directional antennas is that we must identify phase configurations that result in high RSSI or allow for spatial reuse. In the following, we will show that it is possible to create a model that relates the RSSI of the links established from the PHASER mote to the nodes in the testbed. The model digests our understand of how PHASER behaves in environments where there is line-of-sight.

We start by observing that in Figure 7 there an interesting oscillation between low and high quality when link quality is measured using RSSI: the link's RSSI oscillates from -92 dBm to -82 dBm almost periodically. This pattern is the results of how we iterate through the 64 measured antenna configurations in the figure. In order to better understand the relationship between phases and RSSI, we replot the data as a pcolor plot where the rows and columns indicate the phases of antennas A and B while the color indicates the measured RSSI. Figure 9 plots the phase matrices for three nodes in the network. The figure suggests that the patterns of the phase matrices are shifted and scaled version of the same underlying pattern. If the hypothesis is correct, we should be able to reproduce the phase matrices of the other nodes from the base template. Accordingly, assuming that the phase matrix is of size $N \times N$ and using the phase matrix of node 0 as a base template, we can derive the phase matrix PM_i of any other node i in the network. Specifically, the RSSI value of PM_i for phase configuration ϕ_A and ϕ_B can be computed using:

$$PM_i[\phi_A, \phi_B] = o + s \times PM_0[(\phi_A + \phi'_A)\%N, (\phi_B + \phi'_B)\%N]$$

where $\%$ is the modulus operator. The model has four parameters. The ϕ'_A and ϕ'_B parameters shift the base template to better fit the target phase matrix. The offset o and scale s parameters correct for the fact that the nodes may have different RSSI levels as they are located at different distances relative to the receiver.

We wrote a program that fits the model in two steps. First, we find the best phase shift for each antenna that minimizes the squared error between the entries in the considered phase matrix and those in the base template. Since there at most 64 combinations of possible phase shifts, we exhaustively evaluate each one of them. Second, we scale the values in the shifted phase matrix using least square optimizations to account that the phase matrix has a different range of RSSI values due to the nodes being located at different distances from PHASER mote.

Figure 10a details the process of estimating the RSSI at node 1 based on that of node 0. The first shows the original RSSI of nodes 0 and 1. The RSSI of node 1 is estimated by first adjusting the phase of node 0's RSSI and then scaling it as shown in the figure. Figure 10b plots the errors observed when the link quality of nodes 1 – 15 are estimated based on the link quality of node 0. The median errors for all nodes are below 2 dBm suggesting that this approach is effective in accurately capturing the behavior of the links in the network. We have evaluated the model using the five different motes.

Results 5: The phase matrices measured at different receivers from a single PHASER mote have the same underly-

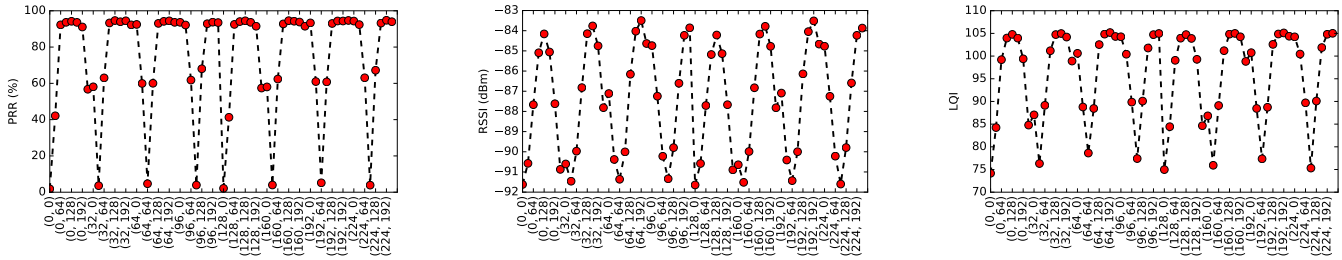

(a) PRR of node 0 (b) RSS of node 0 (c) LQI of node 0

Figure 7: The quality of the link from A+L measured at node 0 using PRR, LQI, and RSS

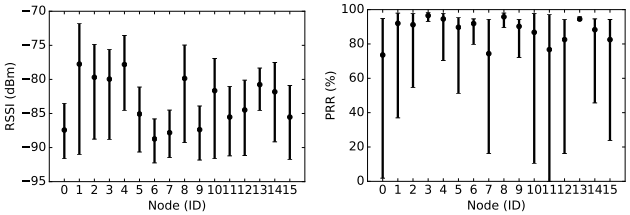

(a) RSSI (b) PRR

Figure 8: The impact of phase configuration changes on links from PHASER A to testbed motes

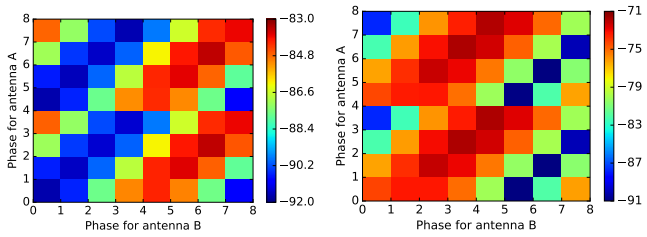

(a) Phase matrix of node 0 (b) Phase matrix of node 1

Figure 9: Phase matrix for different nodes in the testbed for PHASER A.

ing pattern. Picking one the phase matrix of one of the nodes as a template, it is possible to reproduce the phase matrix of any other receiver by shifting and scaling the template with average absolute errors less than 2 dBm.

IV. Related Work

Omnidirectional antennas radiate signals in all directions to create a single radiation pattern. In contrast, smart antennas can use techniques such as beam switching, beam steering, or beam forming to create multiple radiation patterns. Smart antennas can significantly improve link quality [3], network capacity [4], [5], and security [6].

The unique characteristics of WSN application significantly constrain the design of smart antennas particularly in regards to requiring simple signal processing techniques and ease of manufacturing. A number of beam-switched designs have been proposed to address these limitations. A common design is to use electronically switched parasitic element elements as SPIDA [7] and SANTA [8] The two antennas have a central active element that is surrounded

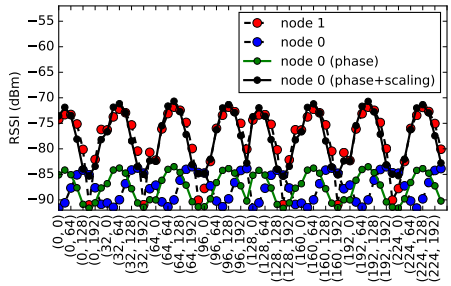

(a) Estimated link quality of node 1 when node 0 is used as a template

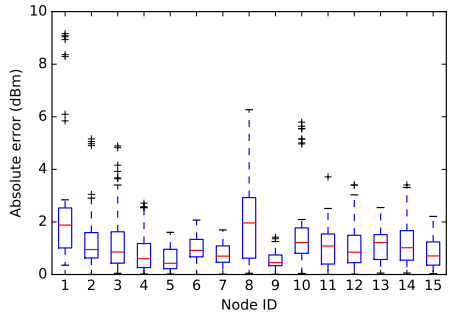

(b) Distribution of absolute errors

Figure 10: A model for phase-shifting directional antennas

by parasitic elements. By grounding or letting the parasitic elements float, the radiation pattern of the antenna can be changed. Zhang *et al.* [9] propose a linearly polarized pattern reconfigurable microstrip parasitic array elements in which four switches are used to reconfigure the radiation pattern. In the [10], a four-beam patch antenna (FBPA) with the goal of miniaturizing directional antenna for WSN node is proposed. FBPA consists of four coaxially fed planar patch antennas arranged in the four lateral faces of a cube that contains the WSN node. The patch that is used for communication can be dynamically changed. Two-element switched beam antenna array has been proposed in [11] and [12]. Directionality is achieved by dynamically controlling which antenna in the array is activated. The above designs have the advantage that they do not require complex signal processing techniques. However, a significant limitation is that a beam switching approach can create only a small number of radiation

patterns depending on the number of antennas or parasitic elements used. This significantly limits the opportunities for improving communication performance. Additionally, the performance of the antennas is affected by the placement of the antennas increasing manufacturing complexity.

In this paper, we present PHASER platform that has two antennas and provides directional communication by programmatically controlling the phases of the signals sent to each antenna. An advantage of PHASER is that it can create numerous antenna patterns each phase being controlled using an 8-bit number for a total of 65,536 possible configurations. This gives more freedom in pattern generation than the beam switching designs presented in the related work. Additionally, PHASER is easier to manufacture as its performance is less susceptible to the geometry of the antenna than the previously discussed approaches.

In spite of the potential benefits of using directional communication in WSNs, there is a paucity of empirical studies that characterize the empirical properties of WSN directional antennas. The closest related works are the in-depth empirical studies performed using the SPIDA antenna [1]. The studies demonstrate the benefits of directional communication and provide insights on how the configuration of the antenna may be changed to improve link quality. The empirical study presented in this paper further quantifies the potential benefits of using directional antennas in WSNs. Our study is complementary to the studies on SPIDA as PHASER and SPIDA use different techniques to improve directional communication. A challenge to using PHASER is that protocols must select the configuration that maximizes link quality or spatial reuse out of a large number of possibility. To tame this complexity, we propose a model that can predict the quality of links from a transmitter accurately.

V. Conclusions

This paper presented the design and empirical evaluation of PHASER. A PHASER has three main components: a low power radio, an RF signal processing core, and two off-the-shelf whip antennas mounted half wavelength apart. The radio signal for each antenna is manipulated to change the radiation pattern of the system. The phase shift can be controlled using an 8-bit value with a resolution of 1.4 degrees. PHASER is well-suited for WSN applications: (1) PHASER introduces minimal energy overhead: the two RF chips add only 0.4 mA which increases the current draw by 1.8% during packet transmission compared to when the CC2420 is used without phase shifting. (2) PHASER requires no additional signal processing and, as a result, low-power and resource constrained microcontrollers may be used in mote designs. (3) PHASER is easy to manufacture.

We have extensively evaluated the performance of five PHASER motes.Our experiments show that changes in the PHASER's phase configuration significantly impact radiation patterns and link quality. Empirical results show that the signal strength of a link may be improved by at least 13 dBm.The results indicate a node may have a spatial reuse index ranging between 40% – 80%. This suggests reuse opportunities are available for a large fraction of the orientations. The spatial reuse index was similar across the tested PHASER prototypes and used antennas. A key challenge of using PHASER antennas is identifying the best configuration that must be used out 65,536 available configurations. We show that quality of links from PHASER share an underlying phase matrix. Accordingly, the phase matrix of any receiver may be reconstructed by phase shifting and scaling a template matrix. The model is computationally efficient and may be used for either simulations or incorporated in protocol stacks.

References

[1] T. Voigt, L. Mottola, and K. Hewage, "Understanding link dynamics in wireless sensor networks with dynamically steerable directional antennas," in *European Conference on Wireless Sensor Network*, 2013.

[2] *UltraCMOS RF Digital Phase Shifter*, Peregrine Semiconductor, 7 2016, dOC-43214-6.

[3] S. Sen, J. Xiong, R. Ghosh, and R. R. Choudhury, "Link layer multicasting with smart antennas: No client left behind," in *International Conference on Network Protocols*, Oct 2008.

[4] S. Yi, Y. Pei, and S. Kalyanaraman, "On the capacity improvement of ad hoc wireless networks using directional antennas," in *International Symposium on Mobile Ad Hoc Networking & Computing*, 2003.

[5] H. N. Dai, "Throughput and delay in wireless sensor networks using directional antennas," in *International Conference on Intelligent Sensors, Sensor Networks and Information*, Dec 2009.

[6] L. Hu and D. Evans, "Using directional antennas to prevent wormhole attacks," in *Annual Network and Distributed System Security Symposium*, Feb 2004.

[7] M. Nilsson, "SPIDA: a direction-finding antenna for wireless sensor networks," in *International Workshop on Real-World Wireless Sensor Networks*, 2010.

[8] K. Prieditis, I. Drikis, and L. Selavo, "Santarray: passive element array antenna for wireless sensor networks," in *Embedded Networked Sensor Systems*, 2010.

[9] S. Zhang, G. H. Huff, J. Feng, and J. T. Bernhard, "A pattern reconfigurable microstrip parasitic array," *IEEE Transactions on Antennas and Propagation*, 2004.

[10] G. Giorgetti, A. Cidronali, S. K. S. Gupta, and G. Manes, "Exploiting low-cost directional antennas in 2.4 GHz IEEE 802.15.4 wireless sensor networks," in *European Conference on Wireless Technologies*, Oct 2007.

[11] D. Leang and A. Kalis, "Smart SensorDVB: sensor network development boards with smart antennas," in *Proceedings of the International Conference on Communications, Circuits and Systems*, 2004.

[12] B. Liang, B. Sanz-Izquierdo, J. C. Batchelor, and A. Bogliolo, "Active FSS enclosed beam-switching node for wireless sensor networks," in *European Conference on Antennas and Propagation*, 2014.